electronics

Article

Iterative Design Algorithm for Robust Disturbance-Rejection Control

Jixuan Li, Pan Yu *, Nike Liu, Henan Zhao and Chunfang Liu

Faculty of Information Technology, Beijing University of Technology, Beijing 100124, China; lijixuan@emails.bjut.edu.cn (J.L.)
* Correspondence: panyu@bjut.edu.cn

Abstract: An iterative design algorithm is developed for robust disturbance–rejection control of uncertain systems with time-varying parameter perturbations in this paper. For more design degrees of freedom, a generalized equivalent-input-disturbance estimator is adopted to approximate the effect of both disturbances and uncertainties. By the bound real lemma, the H_∞ norm is used to evaluate the robust disturbance–rejection performance of the closed-loop uncertain system. To avoid the constraints introduced by the widely used commutative condition, the control gains are divided into two groups and calculated by steps. Further, two robust quadratic stability conditions are derived, and an iterative design algorithm is developed to optimize the robust H_∞ disturbance–rejection performance. Finally, the effectiveness and advantages of the developed method are demonstrated by a case study of a suspension system of modern vehicles.

Keywords: disturbance-rejection; uncertain system; robust control; parameter perturbation; performance optimization

check for updates

Citation: Li, J.; Yu, P.; Liu, N.; Zhao, H.; Liu, C. Iterative Design Algorithm for Robust Disturbance-Rejection Control. *Electronics* **2023**, *12*, 2114. https://doi.org/10.3390/electronics12092114

Academic Editor: Jose Luis Calvo-Rolle

Received: 2 April 2023
Revised: 30 April 2023
Accepted: 4 May 2023
Published: 5 May 2023

1. Introduction

Practical systems often suffer from unknown disturbances and uncertainties. They deteriorate control accuracy and even destabilize the systems [1]. For these reasons, disturbance–rejection control is one of the key issues in control practice.

To improve the disturbance–rejection performance, many strategies have been developed [2,3]. They can be mainly divided into two categories [4]. The passive methods use a common feedback loop to handle multiple control objectives at the same time, which include robust stability, disturbance rejection, noise suppression, etc. By considering the unknown disturbances and uncertainties as an overall disturbance, the active methods introduce an additional loop, specifically for disturbance estimation and suppression control, resulting in better control performance [5,6].

By utilizing all the information of system states, the uncertainty and disturbance estimator is developed by assuming any signals can be properly approximated by filtering [7,8]. The disturbance observer in the frequency domain is composed of a filter and an inverse dynamic of a nominal plant [9]. It may be a bit tricky to design the filter to simultaneously fulfill causality, robust stability, and disturbance–rejection performance. Some techniques were performed to ease the design [10]. The disturbance observer in the time domain is built on known disturbance models [11,12]. The extended-state observer is applicable to more general systems, which is another effective method for integral systems with matched disturbances or mismatched disturbances that can be transformed into matched ones [13]. The generalized extended-state observer is applicable to general systems. However, a static or dynamic compensation gain is usually required for mismatched disturbance [14,15].

Focusing on the influence of disturbances or uncertainties on the system output, the equivalent-input-disturbance (EID) approach is developed for simple and effective disturbance–rejection control [16]. An EID is a virtual disturbance defined on the control input, which has the same effect on the system output as the real disturbances do. Since the EID approach provides an estimate of the disturbances or uncertainties on the control input, it does not require the disturbance compensation gain. That is to say, it is usually useful for both matched and mismatched disturbances [17,18]. Moreover, only output information is required for EID estimation. It uses only output information and does not need the direct availability of system states, the disturbance model, the differentiation of measured outputs, or an inverse dynamics of a plant. So, it is easy to implement.

In engineering practice, it is difficult to obtain a precise mathematical model of a physical system, owning to parameter perturbations, modeling errors, unmodeled dynamics, and other factors. Moreover, as explained by [19], the uncertainties impact the disturbance–rejection control performance. So, it is vital and necessary to design a robust controller with a prescribed disturbance–rejection performance index. A robust controller was designed for an uncertain system [20], but some constraints were introduced by using the commutative condition. By taking the uncertainties into account, a parameter design method was developed for an improved EID-based system in [21], but it cannot guarantee disturbance–rejection performance. A disturbance–rejection control method with H_∞ performance was developed in [22], but it was designed in the frequency domain. Some expertise may be needed to select the weighting functions.

In this paper, an iterative design algorithm is developed for an uncertain system with unknown disturbances. The EID approach is applied to handle the disturbances. The Luenberger observer is constructed to reproduce the system states. Then, a feedback controller is designed to stabilize the closed-loop uncertain system. Finally, an optimization design algorithm is given. The major contributions of this paper are given as below.

1. A generalized EID estimator (GEID) with a general filter is developed, which enables handling disturbances in a specified frequency range.
2. For the sake of less conservatism, the control gains are divided into two groups and designed in steps.
3. Two robust quadratic stability conditions are derived in terms of linear matrix inequalities (LMIs), which guarantee the prescribed H_∞ performance of the closed-loop uncertain system.
4. An iterative design algorithm is presented to optimize the H_∞ performance of the closed-loop uncertain control system.

The remainder of this paper is organized as below. The system configuration is explained in Section 2. Section 3 analyzes the dynamics of the GEID-based disturbance–rejection control system. Section 4 presents conditions with prescribed disturbance–rejection performance. A design procedure is presented in Section 5. The validity and superiority of the developed method are demonstrated by Section 6. Section 7 concludes this paper. Further, a consolidated list of variables and acronyms in this paper is given by two tables in Appendix A.

In this paper, $\mathbb{R}^{m\times p}$ denotes the set of $m \times p$ real matrices; I_n denotes an identity matrix of size n; I and 0 stand for identity and zero matrices with compatible dimensions, respectively; P^{T} and P^{-1} denote the transpose and inverse of a matrix P, respectively; $u(s)$ denotes the Laplace transform of a time signal $u(t)$; the time t and the complex frequency s are omitted when the content is clear; $G_{uy}(s)$ denotes the transfer matrix from $y(s)$ to $u(s)$; $\|G\|_\infty$ denotes the H_∞ norm of the transfer matrix $G(s)$; $[Q]_s$ denotes $Q + Q^{\mathrm{T}}$; and a symmetric matrix $\begin{bmatrix} A & B \\ B^{\mathrm{T}} & C \end{bmatrix}$ is denoted by $\begin{bmatrix} A & B \\ \star & C \end{bmatrix}$.

2. Configuration of GEID-Based Disturbance–Rejection Control System

Consider an uncertain plant subject to an exogenous disturbance.

$$\begin{cases} \dot{x}(t) = [A + \Delta A(t)]x(t) + Bu(t) + B_f f(t), \\ y(t) = [C + \Delta C(t)]x(t) + Du(t), \end{cases} \tag{1}$$

where $x(t) \in \mathbb{R}^n$, $u(t) \in \mathbb{R}^p$, $y(t) \in \mathbb{R}^q$ are the state, input, and output of the plant, respectively; $f(t) \in \mathbb{R}^m$ is an unknown disturbance; A, B, B_f, C, and D are dimensioned real constant matrices; and $\Delta A(t)$ and $\Delta C(t)$ are time-varying uncertainties in the following general structure

$$\begin{bmatrix} \Delta A(t) \\ \Delta C(t) \end{bmatrix} = \begin{bmatrix} N_A \\ N_C \end{bmatrix} E(t) M, \tag{2}$$

where M, N_A, and N_C are known real constant matrices; and $E(t)$ is a time-varying real function matrix with Luenberger measurable elements while satisfying

$$E^{\mathrm{T}}(t)E(t) \leq I, \ \ \forall t > 0. \tag{3}$$

Note the uncertainties considered in the control system appear only in the state matrix A and the output matrix C.

The time-varying parameter perturbations of the system matrix and output matrix are considered in this paper. Many scenarios fall into this case [23].

Assumption 1. *Assumption: The system (1) is controllable and observable.*

Assumption 2. *Assumption: The disturbance $f(t)$ is bounded, i.e.,*

$$\|f(t)\|_2 \leq f_m. \tag{4}$$

where $\|f(t)\|_2$ is the 2-norm of $f(t)$ and f_m is an unknown upper bound.

Assumption 1 is standard for system design [24], and Assumption 2 usually holds in practice.

As illustrated in Figure 1, the control structure of the developed GEID-based robust control system includes a plant, a state observer, a GEID estimator, and a state-feedback controller based on observed states.

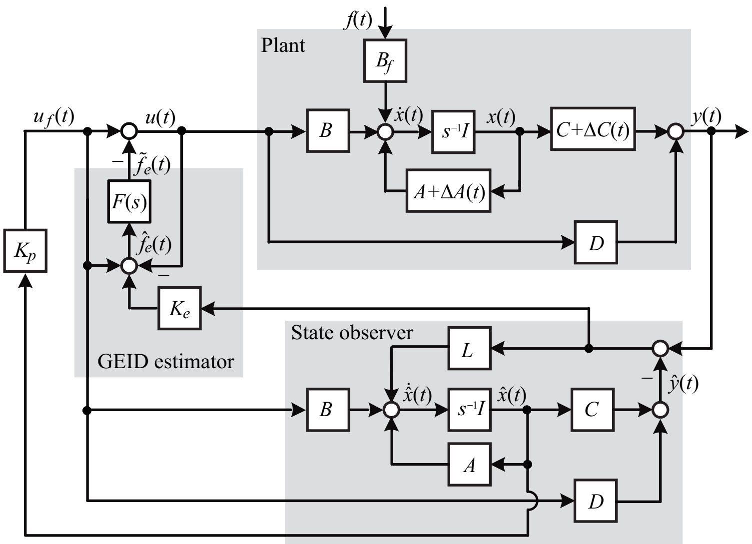

Figure 1. Robust disturbance–rejection control system with generalized equivalent-input-disturbance (GEID) estimator.

Since $f(t)$ is unknown, lump them as $\bar{f}(t)$.

$$\bar{f}(t) = B_f f(t). \tag{5}$$

When the full-state is not available or too costly, a state observer with full order is constructed to produce the states of the plant (1). Some design strategies of the state observer were talked about in [25,26]. In this paper, the observer system is viewed as the ideal dynamic of the real plant (1)

$$\begin{cases} \dot{\hat{x}}(t) = A\hat{x}(t) + Bu_f(t) + L[y(t) - \hat{y}(t)], \\ \hat{y}(t) = C\hat{x}(t) + Du_f(t), \end{cases} \tag{6}$$

where $\hat{x}(t) \in \mathbb{R}^n$, $u_f(t)$, $\hat{y}(t)$ are the state, input, and output of the observer, respectively; and L is the observer gain to be determined.

The EID approach is adopted for active disturbance rejection control. As analyzed in [16], the filter $F(s)$ is of great importance to the performance. For disturbances in a low-frequency range, a first-order low-pass filter satisfying the following condition is good enough.

$$F(j\omega) \to I, \forall\omega \in [0, \omega_r], \tag{7}$$

where the angular frequency ω_r is the bandwidth of the low-pass filter $F(s)$ and determined by the disturbance–rejection control design. However, when there exist tight constrains on control bandwidth [19] or specific performance requirements on the middle-frequency range, a general filter is necessary. Superior to the conventional EID one, the GEID approach is able to estimate disturbances of a more general frequency range by a general filter.

In this paper, a GEID estimator is adopted for EID estimation, where a control gain K_e is introduced to adjust the control performance and a general filter is used for a general design task. A state–space representation of $F(s)$ is

$$\begin{cases} \dot{x}_F(t) = A_F x_F(t) + B_F \hat{f}_e(t), \\ \tilde{f}_e(t) = C_F x_F(t), \end{cases} \tag{8}$$

where $x_F(t) \in \mathbb{R}^{n_f}$ is the state of the filter; and $\hat{f}_e(t)$, $\tilde{f}_e(t)$ are the unfiltered and filtered estimates of the EID, respectively. For simplicity, denote

$$\begin{aligned} x_e(t) &= x_F(t), \quad A_e = A_F + B_F C_F, \\ B_e &= B_F K_e, \quad C_e = C_F. \end{aligned} \tag{9}$$

Further, an equivalent description of the GEID estimator is

$$\begin{cases} \dot{x}_e(t) = (A_e - B_e D C_e) x_e(t) + B_e C \tilde{x}(t) + B_e \Delta C(t) x(t), \\ \tilde{f}_e(t) = C_e x_e(t). \end{cases} \tag{10}$$

When B_F is selected to have full column rank, we have $K_e = B_F^+ B_e$ with B_F^+ being the Moore-Penrose generalized inverse of B_F. In the sequel, calculating K_e is performed by designing B_e.

Based on the observed state $\hat{x}(t)$, the original state-feedback control law is

$$u_f(t) = K_p \hat{x}(t), \tag{11}$$

where K_p is the feedback control gain to be determined. It is used to stabilize the controlled system.

By introducing a degree of freedom in the inner loop for disturbance estimation and compensation, the new control law is

$$u(t) = -\tilde{f}_e(t) + u_f(t). \tag{12}$$

3. Dynamics of GEID-Based Control System

Define

$$\tilde{x}(t) = x(t) - \hat{x}(t), \tag{13}$$

and

$$\tilde{y}(t) = y(t) - \hat{y}(t) = C\tilde{x}(t) + \Delta C(t) x(t) + D[u(t) - u_f(t)]. \tag{14}$$

According to (8), (12), and (14), we have

$$\tilde{y}(t) = C\tilde{x}(t) + \Delta C(t)x(t) - DC_e x_e(t). \tag{15}$$

Substitution of (11) into (6) gives

$$\dot{\hat{x}}(t) = (A + BK_p)\hat{x}(t) + L\tilde{y}(t). \tag{16}$$

Combining (1) and (6) yields

$$\dot{\tilde{x}}(t) = \Delta A(t)x(t) - L\Delta C(t)x(t) + (A - LC)\tilde{x}(t) - (B - LD)\tilde{f}_e(t) + B_f f(t). \tag{17}$$

Define

$$\varphi(t) = [x^{\mathrm{T}}(t)\ \ \tilde{x}^{\mathrm{T}}(t)\ \ x_e^{\mathrm{T}}(t)]^{\mathrm{T}}.$$

From (11) to (17), we have the following state–space description for the closed-loop uncertain control system in Figure 1:

$$\begin{cases} \dot{\varphi}(t) = (\bar{A}^{\varphi} + \Delta\bar{A}^{\varphi})\varphi(t) + \bar{B}^{\varphi}\bar{f}, \\ y(t) = (\bar{C}^{\varphi} + \Delta\bar{C}^{\varphi})\varphi(t), \end{cases} \tag{18}$$

where

$$\begin{aligned} &\bar{A}^{\varphi} = \begin{bmatrix} A + BK_P & -BK_P & 0 \\ 0 & A - LC & -(B - LD)C_e \\ 0 & B_e C & A_e - B_e DC_e \end{bmatrix} \\ &\Delta\bar{A}^{\varphi} = \begin{bmatrix} \Delta A(t) & 0 & 0 \\ \Delta A(t) - L\Delta C(t) & 0 & 0 \\ B_e \Delta C(t) & 0 & 0 \end{bmatrix}, \bar{B}^{\varphi} = \begin{bmatrix} I \\ I \\ 0 \end{bmatrix} \\ &C^{\varphi} = \begin{bmatrix} C + DK_p & -DK_p & 0 \end{bmatrix}, \quad \Delta\bar{C}^{\varphi}(t) = \begin{bmatrix} \Delta C(t) & 0 & 0 \end{bmatrix}. \end{aligned} \tag{19}$$

It is clear that the separation theorem cannot be used due to the parameter uncertainties, and the control gains to be determined scatter in the system matrix. To be specific, the feedback control gain K_p is located on the right-hand side of some elements, while the control gains L and B_e of the observer and GEID estimator are related to the right-hand side.

Inspired by [27], to reduce the conservatism of parameter design by removing the constraints from the widely used commutative condition, the control gains K_p, L, and K_e of the feedback controller, the state observer, and the GEID estimator are divided into two groups, K_p and (L, K_e). Additionally, they are designed by steps.

First, when K_p is assigned prior to L and B_e, the state–space model (18) and (19) is used for system design. For this purpose, rewrite

$$\begin{cases} \bar{A}^{\varphi} = \hat{A}^{\varphi} - \hat{L}\hat{C}, \quad \bar{C}^{\varphi} = \begin{bmatrix} C + DK_p & \bar{C}_1^{\varphi} \end{bmatrix}, \\ \Delta\bar{A}^{\varphi} = \bar{N}_A^{\varphi} E(t)\bar{M}^{\varphi}, \quad \Delta\bar{C}^{\varphi}(t) = N_C E(t)\bar{M}^{\varphi}, \end{cases} \tag{20}$$

where

$$\begin{aligned} &\hat{A}^{\varphi} = \begin{bmatrix} A_K & \hat{A}_1^{\varphi} \\ 0 & A_{\bar{L}} \end{bmatrix}, \quad A_{\bar{L}} = \begin{bmatrix} A & -BC_e \\ 0 & A_e \end{bmatrix}, \quad \hat{L} = \begin{bmatrix} 0 \\ \bar{L} \end{bmatrix}, \quad \bar{L} = \begin{bmatrix} L \\ -B_e \end{bmatrix} \\ &A_K = A + BK_p, \quad \hat{A}_1^{\varphi} = \begin{bmatrix} -BK_p & 0 \end{bmatrix} \\ &\hat{C}^1 = \begin{bmatrix} C & -DC_e \end{bmatrix}, \quad C_1^{\varphi} = \begin{bmatrix} -DK_p & 0 \end{bmatrix}, \quad \hat{C} = \begin{bmatrix} 0 & \hat{C}^1 \end{bmatrix} \\ &\bar{N}_A^{\varphi} = \hat{N}_A^{\varphi} - \hat{L}N_C, \quad \hat{N}_A^{\varphi} = \begin{bmatrix} N_A \\ \hat{N}_{A1}^{\varphi} \end{bmatrix}, \quad \hat{N}_{A1}^{\varphi} = \begin{bmatrix} N_A \\ 0 \end{bmatrix}, \quad \bar{M}^{\varphi} = \begin{bmatrix} M & 0 \end{bmatrix}. \end{aligned} \tag{21}$$

On the other hand, let

$$\theta(t) = [\hat{x}^{\mathrm{T}}(t) \;\; \tilde{x}^{\mathrm{T}}(t) \;\; x_e^{\mathrm{T}}(t)]^{\mathrm{T}}.$$

The closed-loop uncertain control system can also be represented by

$$\begin{cases} \dot{\theta}(t) = (\bar{A}^{\theta} + \Delta\bar{A}^{\theta})\theta(t) + \bar{B}^{\theta}\bar{f}, \\ y(t) = (\bar{C}^{\theta} + \Delta\bar{C}^{\theta})\theta(t), \end{cases} \tag{22}$$

where

$$\begin{aligned} \bar{A}^{\theta} &= \begin{bmatrix} A + BK_p & LC & -LDC_e \\ 0 & A - LC & -(B - LD)C_e \\ 0 & B_eC & A_e - B_eDC_e \end{bmatrix}, \quad \bar{B}^{\theta} = \begin{bmatrix} 0 \\ I \\ 0 \end{bmatrix} \\ \Delta\bar{A}^{\theta} &= \begin{bmatrix} L\Delta C(t) & L\Delta C(t) & 0 \\ \Delta A(t) - L\Delta C(t) & \Delta A(t) - L\Delta C(t) & 0 \\ B_e\Delta C(t) & B_e\Delta C(t) & 0 \end{bmatrix} \\ \bar{C}^{\theta} &= \begin{bmatrix} C + DK_p & C & 0 \end{bmatrix}, \quad \Delta\bar{C}^{\theta}(t) = \begin{bmatrix} \Delta C(t) & \Delta C(t) & 0 \end{bmatrix}. \end{aligned} \tag{23}$$

Similarly, rewrite

$$\begin{cases} \bar{A}^{\theta} = \hat{A}^{\theta} - \hat{L}\hat{C}, \quad \bar{C}^{\theta} = \begin{bmatrix} C + DK_p & \bar{C}_1^{\theta} \end{bmatrix}, \\ \Delta\bar{A}^{\theta} = \bar{N}_A^{\theta}E(t)\bar{M}^{\theta}, \quad \Delta\bar{C}^{\theta}(t) = N_C E(t)\bar{M}^{\theta}, \end{cases} \tag{24}$$

where $\hat{L}$, $\hat{C}$ are defined in (21), and

$$\begin{aligned} \hat{A}^{\theta} &= \begin{bmatrix} A_K & \hat{A}_1^{\theta} \\ 0 & A_{\bar{L}} \end{bmatrix}, \quad \hat{A}_1^{\theta} = \begin{bmatrix} LC & -LDC_e \end{bmatrix}, \quad \bar{C}_1^{\theta} = \begin{bmatrix} C & 0 \end{bmatrix} \\ \bar{N}_A^{\theta} &= \begin{bmatrix} LN_C \\ \hat{N}_{A1}^{\theta} \end{bmatrix}, \quad \hat{N}_{A1}^{\theta} = \begin{bmatrix} N_A - LN_C \\ B_eN_C \end{bmatrix} \\ \bar{M}^{\theta} &= \begin{bmatrix} M & \bar{M}_1^{\theta} \end{bmatrix}, \quad \bar{M}_1^{\theta} = \begin{bmatrix} M & 0 \end{bmatrix}. \end{aligned} \tag{25}$$

Further, for the closed-loop uncertain control system in Figure 1, the transfer matrix $G(s)$ from $\bar{f}$ to y can be written by $G_{y\bar{f}}^{\varphi}(s)$ or $G_{y\bar{f}}^{\theta}(s)$, where

$$G_{y\bar{f}}^{\varphi}(s) = (\bar{C}^{\varphi} + \Delta\bar{C}^{\varphi})[sI - (\bar{A}^{\varphi} + \Delta\bar{A}^{\varphi})]^{-1}\bar{B}^{\varphi}\bar{f}, \tag{26}$$

$$G_{y\bar{f}}^{\theta}(s) = (\bar{C}^{\theta} + \Delta\bar{C}^{\theta})\,[sI - (\bar{A}^{\theta} + \Delta\bar{A}^{\theta})]^{-1}\bar{B}^{\theta}\bar{f}. \tag{27}$$

4. Design of GEID-Based Control System

To facilitate the presentation, we recall the following lemmas.

Lemma 1 (Bounded real lemma [28])**.** *Given $G(s) = (A, B, C, D)$, the following two statements are equivalent:*

1. *The system matrix A is stable and $\|G\|_{\infty} < \gamma$.*
2. *There exists a symmetric, positive–definite matrix P, such that the following inequality holds.*

$$\begin{bmatrix} A^{\mathrm{T}}P + PA & PB & C^{\mathrm{T}} \\ B^{\mathrm{T}}P & -\gamma I & D^{\mathrm{T}} \\ C & 0 & -\gamma I \end{bmatrix} < 0. \tag{28}$$

Lemma 2 ([29])**.** *For given dimensioned matrices $N = N^{\mathrm{T}}$, H, F, and any $E(t)$ satisfying*

$$E^{\mathrm{T}}(t)E(t) \leq I, \tag{29}$$

the following inequality holds

$$N + HE(t)F + F^{\mathrm{T}}E^{\mathrm{T}}(t)H^{\mathrm{T}} < 0, \tag{30}$$

if and only if there is an positive constant ε, such that

$$N + \varepsilon HH^{\mathrm{T}} + \varepsilon^{-1}F^{\mathrm{T}}F < 0. \tag{31}$$

Lemma 3 (Schur complement argument [30])**.** *For any real symmetric matrix Σ,*

$$\Sigma = \begin{bmatrix} S_{11} & S_{12} \\ \star & S_{22} \end{bmatrix},$$

we have the following equivalent assertion:

1. $\Sigma < 0$;
2. $S_{11} < 0$ *and* $S_{22} - S_{12}^{T}S_{11}^{-1}S_{12} < 0$;
3. $S_{22} < 0$ *and* $S_{11} - S_{12}S_{22}^{-1}S_{12}^{T} < 0$.

With known K_p, a robust stability condition together with the gains of (L, K_e), are given as below, which guarantees the H_∞ disturbance–rejection performance of the closed-loop uncertain control system, i.e.,

$$\|G\|_\infty < \gamma. \tag{32}$$

Theorem 1. *For a prescribed positive scalar γ, select (A_e, C_e), and give control gain K_p if there exist a symmetric, positive–definite matrix P, a dimensioned matrix W_1, and positive constants ε_1 and ε_2, such that the following inequalities hold,*

$$\begin{bmatrix} \Phi_1 & \varepsilon_1(\bar{M}^\varphi)^{\mathrm{T}} & \Phi_2 \\ \star & -\varepsilon_1 & 0 \\ \star & \star & -\varepsilon_1 \end{bmatrix} < 0, \tag{33}$$

$$\begin{bmatrix} \Phi_1 & P\bar{B}^\varphi & (\bar{C}^\varphi)^{\mathrm{T}} & \varepsilon_2(\bar{M}^\varphi)^{\mathrm{T}} & \Phi_2 \\ \star & -\gamma I & 0 & 0 & 0 \\ \star & \star & -\gamma I & 0 & N_C \\ \star & \star & \star & -\varepsilon_2 & 0 \\ \star & \star & \star & \star & -\varepsilon_2 \end{bmatrix} < 0, \tag{34}$$

Then the GEID-based closed-loop uncertain control system in Figure 1 is robust stabilized and satisfies the robust H_∞ performance condition (32). The blocks are given by

$$\begin{aligned} \Phi_1 &= \begin{bmatrix} P_1 A_K & P_1 \hat{A}_1^\varphi \\ 0 & P_2 A_{\bar{L}} - W_1 \hat{C}^1 \end{bmatrix}_s \\ \Phi_2 &= \begin{bmatrix} P_1 N_A \\ P_2 \hat{N}_{A1}^\varphi - W_1 N_C \end{bmatrix}, \ P = \begin{bmatrix} P_1 & 0 \\ 0 & P_2 \end{bmatrix}. \end{aligned} \tag{35}$$

Further, the gains of the state observer and GEID estimator are, respectively,

$$L = [I_n \ \ 0]P^{-1}W_1, \ \ K_e = B_F^{+}\left[0 \ \ I_{n_f}\right]P^{-1}W_1. \tag{36}$$

where B_F^{+} is the Moore-Penrose generalized inverse of B_F.

Proof of Theorem 1. Choose a candidate of the Lyapunov functional

$$V(\varphi(t),t) = \varphi^{\mathrm{T}}(t)P\varphi(t), \tag{37}$$

where P is a symmetric, positive–definite matrix, which is defined in (35).

The derivative of $V(\varphi(t),t)$ along the GEID-based closed-loop uncertain control system (18) is

$$\dot{V}(t) = \varphi^{\mathrm{T}}(t)\left[P\bar{A}^{\varphi} + P\bar{N}_A^{\varphi}E(t)\bar{M}^{\varphi}\right]_s \varphi(t). \tag{38}$$

If

$$\left[P\bar{A}^{\varphi} + P\bar{N}_A^{\varphi}E(t)\bar{M}^{\varphi}\right]_s < 0, \tag{39}$$

Then the system (18) is robust stabilized. Application of Lemma 2 to (39) shows that the GEID-based uncertain closed-loop control system is robust stable if the following matrix inequality holds.

$$[P\bar{A}^{\varphi}]_s + \varepsilon_1^{-1}P\bar{N}_A^{\varphi}\left(\bar{N}_A^{\varphi}\right)^{\mathrm{T}}P + \varepsilon_1(\bar{M}^{\varphi})^{\mathrm{T}}\bar{M}^{\varphi} < 0, \tag{40}$$

where ε_1 is a positive scalar. By Lemma 3, (40) is equivalent to the following inequality.

$$\begin{bmatrix} [P\bar{A}^{\varphi}]_s & \varepsilon_1(\bar{M}^{\varphi})^{\mathrm{T}} & P\left(\bar{N}_A^{\varphi}\right) \\ \star & -\varepsilon_1 & 0 \\ \star & \star & -\varepsilon_1 \end{bmatrix} < 0. \tag{41}$$

Substitution of (35) and (36) into (33) gives (41). Therefore, the closed-loop system is stabilized.

On the other hand, by Lemma 2 and Lemma 3, a combination of (34) and (36) yields the following inequality

$$\begin{bmatrix} [P(\bar{A}^{\varphi} + \Delta\bar{A}^{\varphi})]_s & P\bar{B}^{\varphi} & (\bar{C}^{\varphi})^{\mathrm{T}} + (\Delta\bar{C}^{\varphi})^{\mathrm{T}} \\ \star & -\gamma I & 0 \\ \star & \star & -\gamma I \end{bmatrix} < 0,$$

which corresponds to the performance index (32) of the closed-loop uncertain control system (18) by Lemma 1. This completes the proof. □

On the other hand, with known $(L\ , K_e)$, the following theorem gives a design method for K_p and guarantees the prescribed H_∞ disturbance–rejection performance index (32).

Theorem 2. *For prescribed positive scalar γ , selected (A_e, C_e), and given control gains $(L\ , K_e)$, if there exist a symmetric, positive–define matrix $\bar{P}$, a dimensioned matrix W_2, and positive constants ε_3 and ε_4, such that the following inequalities hold,*

$$\begin{bmatrix} \Theta_1 & \bar{P}\left(\bar{M}^{\theta}\right)^{\mathrm{T}} & \varepsilon_3\bar{N}_A^{\theta} \\ \star & -\varepsilon_3 & 0 \\ \star & \star & -\varepsilon_3 \end{bmatrix} < 0, \tag{42}$$

$$\begin{bmatrix} \Theta_1 & \bar{B}^{\theta} & \bar{P}\left(\bar{C}^{\theta}\right)^{\mathrm{T}} & \bar{P}\left(\bar{M}^{\theta}\right)^{\mathrm{T}} & \varepsilon_4\bar{N}_A^{\theta} \\ \star & -\gamma I & 0 & 0 & 0 \\ \star & \star & -\gamma I & 0 & \varepsilon_4 N_C \\ \star & \star & \star & -\varepsilon_4 & 0 \\ \star & \star & \star & \star & -\varepsilon_4 \end{bmatrix} < 0, \tag{43}$$

where

$$\Theta_1 = \begin{bmatrix} A\bar{P}_1 + BW_2 & \hat{A}_1^\theta \bar{P}_2 \\ 0 & A_{\bar{L}}\bar{P}_2 - \bar{L}\hat{C}^1\bar{P}_2 \end{bmatrix}_s, \quad \bar{P} = \begin{bmatrix} \bar{P}_1 & 0 \\ 0 & \bar{P}_2 \end{bmatrix}, \tag{44}$$

then the GEID-based closed-loop uncertain control system in Figure 1 is stable and satisfies the robust H_infty performance condition (42). Further, the gain of the feedback controller is given by

$$K_p = W_2\bar{P}_1^{-1}. \tag{45}$$

Proof of Theorem 2. A candidate of Lyapunov functional is selected as

$$V(\theta(t), t) = \theta^{\mathrm{T}}(t)\bar{P}^{-1}\theta(t), \tag{46}$$

where $\bar{P}^{-1}$ is a positive–definite, symmetric matrix defined in (44).

The derivative of $V(\theta(t), t)$ along the GEID-based closed-loop uncertain control system (22) is

$$\dot{V}(t) = \theta^{\mathrm{T}}(t)\left[\bar{P}^{-1}\bar{A}^\theta + \bar{P}^{-1}\bar{N}_A^\theta E(t)\bar{M}^\theta\right]_s \theta(t). \tag{47}$$

If

$$\left[\bar{P}^{-1}\bar{A}^\theta + \bar{P}^{-1}\bar{N}_A^\theta E(t)\bar{M}^\theta\right]_s < 0, \tag{48}$$

then the GEID-based closed-loop uncertain control system (22) is robust stable. By Lemma 2, if and only if there exists a positive constant ε_3, such that

$$\left[\bar{P}^{-1}\bar{A}^\theta\right]_s + \varepsilon_3^{-1}\bar{P}^{-1}\bar{N}_A^\theta\left(\bar{N}_A^\theta\right)^{\mathrm{T}}\bar{P}^{-1} + \varepsilon_3\left(\bar{M}^\theta\right)^{\mathrm{T}}\bar{M}^\theta < 0, \tag{49}$$

then (48) holds. Pre- and post-multiplying the term on the left-hand side of (49) by $\bar{P}$ gives

$$\left[\bar{A}^\theta\bar{p}\right]_s + \varepsilon_3\bar{N}_A^\theta\left(\bar{N}_A^\theta\right)^{\mathrm{T}} + \varepsilon_3^{-1}\bar{p}\left(\bar{M}^\theta\right)^{\mathrm{T}}\bar{M}^\theta\bar{p} < 0. \tag{50}$$

According to Lemma 3, (50) is equivalent to the following inequality.

$$\begin{bmatrix} [\bar{A}^\theta\bar{P}]_s & \bar{P}(\bar{M}^\theta)^{\mathrm{T}} & \varepsilon_3(\bar{N}_A^\theta) \\ \star & -\varepsilon_3 & 0 \\ \star & \star & -\varepsilon_3 \end{bmatrix} < 0. \tag{51}$$

Substituting (44) into (42) yields (51). Therefore, the closed-loop system is robust stabilized.

On the other hand, according to Lemma 2 and Lemma 3, substituting (44) into (43) gives the following inequality

$$\begin{bmatrix} [(\bar{A}^\theta + \Delta\bar{A}^\theta)\bar{P}]_s & \bar{B}^\theta & \left[\bar{P}(\bar{C}^\theta + \Delta\bar{C}^\theta)^{\mathrm{T}}\right]_s \\ \star & -\gamma I & 0 \\ \star & \star & -\gamma I \end{bmatrix} < 0.$$

By Lemma 1, the above inequality is actually the performance index (32) of the closed-loop system (22). This completes the proof. □

Remark 1. *Both Theorems 1 and 2 are robust stability conditions for the GEID-based closed-loop uncertain control system shown in Figure 1, which ensure the prescribed H_∞ disturbance–rejection performance (32). When the gain K_p of the feedback controller is known, Theorem 1 is applied to calculate the gains $(L,\ K_e)$ of the observer and GEID; when $(L,\ K_e)$ are known, Theorem 2 is adopted to compute K_p.*

Remark 2. *As for how to obtain a possible gain K_p for Theorem 1 or a set of gains $(L,\ K_e)$ for Theorem 2, as explained in [27], the gains K_p which make the system matrix $\bar{A}^\varphi$ in (18) and $\bar{A}^\theta$ in (22) Hurwitz, respectively, are appropriate. Note*

$$\begin{bmatrix} A - LC & -(B - LD)C_e \\ B_eC & A_e - B_eDC_e \end{bmatrix} = A_{\bar{L}} - \bar{L}\hat{C}^1.$$

where $A_{\bar{L}}$, $\bar{L}$, and $\hat{C}^1$ are defined in (21). Therefore, a proper K_p can be obtained by making A_K in (18) Hurwitz, and an appropriate set of $(L,\ K_e)$ can be gained to such that $A_{\bar{L}} - \bar{L}\hat{C}^1$ is Hurwitz.

5. Design Algorithm

Summarizing the aforementioned results gives the following iterative design procedure for the GEID-based uncertain control system, which optimizes the robust disturbance–rejection performance by minimize the H_∞ performance index γ in (32). Further, the flowchart is shown in Figure 2.

Step 1: Choose an appropriate general filter $F(s) = (A_F, B_F, C_F)$, with B_F being full column rank for the GEID estimator (8).
Step 2: Calculate A_e and C_e according to (9).
Step 3: Select an initial performance index γ_0 and let $\gamma = \gamma_0$.
Step 4: Determine an initial value for the control gains K_p or (L, K_e). If the initial value is determined for K_p, go to Step 5; otherwise, go to Step 6.
Step 5: For known K_p, check if LMIs (33) and (34) in Theorem 1 have feasible solutions. If yes, calculate the resultant (L, K_e) by (36), and go to Step 7; if not, when $\gamma = \gamma_0$, go to Step 3 to increase the initial value γ_0. Otherwise, go to Step 8.
Step 6: For known (L, K_e), check if LMIs (42) and (43) in Theorem 2 have feasible solutions. If yes, calculate the resultant K_p by (45), and go to Step 7; if not, when $\gamma = \gamma_0$, go to Step 3 to increase the initial value γ_0. Otherwise, go to Step 8.
Step 7: Let $\gamma = \gamma - \gamma_\delta$, where γ_δ is the decrease step. Determine the parameters to be optimized. If the known K_p is used to optimize the gains (L, K_e), go to Step 5; otherwise, go to Step 6.
Step 8: Adopt $\{K_p, (L, K_e)\}$ and γ of the previous step as the finial gains and H_∞ performance index, and end the design.

Remark 3. *In Step 1, the selection of $F(s)$ is based on the frequency range of disturbance–rejection control. In Step 4, many methods can be used to obtain the initial values of K_p and (L, K_e), such as the pole placement and linear quadratic regulator (LQR). In Step 7, it may take some trial and error to determine the iteration step and the iteration optimization sequence of control gains. For example, when (L, K_e) are too large, it is inappropriate to use them to optimize K_p. The computation time of the developed design algorithm is usually dependent on the iterative search process. The computation time with a small iteration step is usually greater than that with a large one. In other words, there is a trade-off between the computation complexity and robust disturbance–rejection performance.*

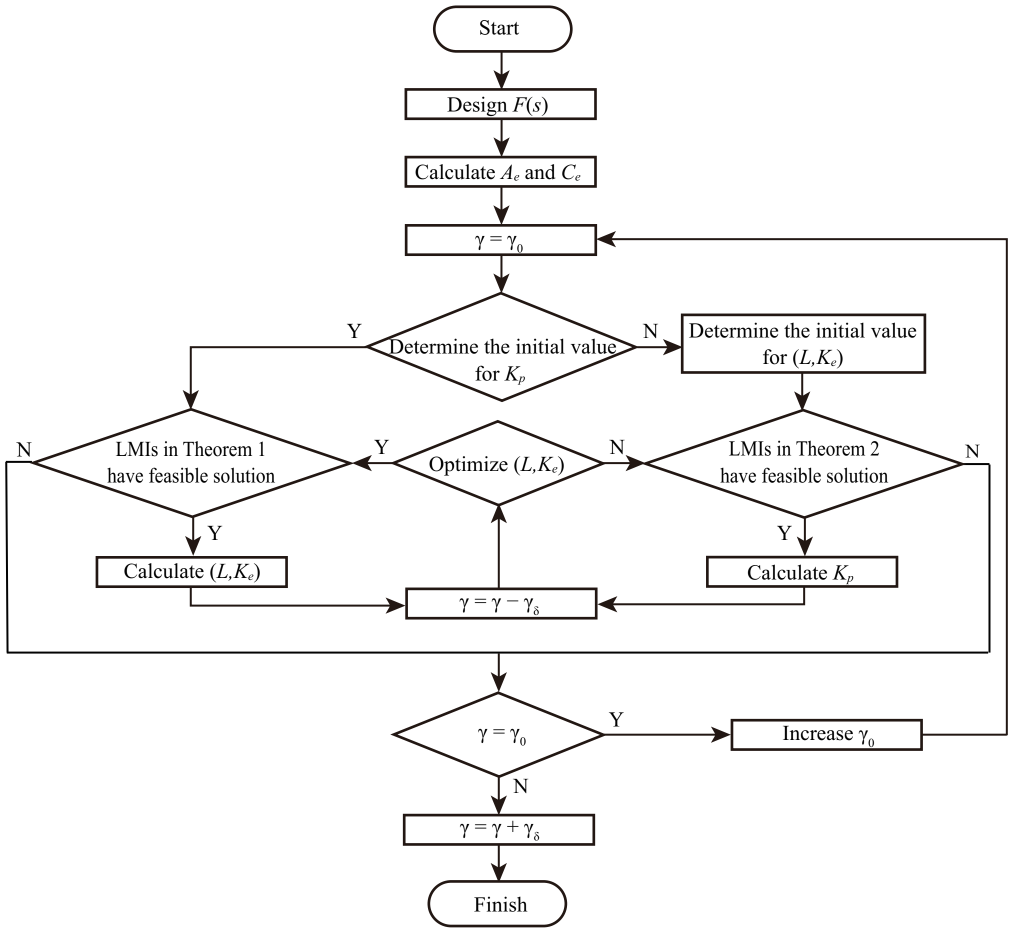

Figure 2. Flowchart of the algorithm.

6. Case Study

In this section, a suspension system of modern vehicles is used to validate the developed method, which is responsible for ride safety and comfor. By the ISO2361, in the vertical direction, the human body is sensitive to vibrations within [4 Hz, 8 Hz]. So, the developed method is used to deal with the road disturbances over this range.

6.1. System Design

The parameters of the suspension system of a quarter-car model are

$$\left\{\begin{array}{l} A=\begin{bmatrix} 0 & 0 & 1 & -1 \\ 0 & 0 & 0 & 1 \\ -\frac{k_s}{m_s} & 0 & -\frac{c_s}{m_s} & \frac{c_s}{m_s} \\ \frac{k_s}{m_u} & -\frac{k_t}{m_u} & \frac{c_s}{m_u} & -\frac{c_s+c_t}{m_u} \end{bmatrix}, B=\begin{bmatrix} 0 \\ 0 \\ \frac{1}{m_s} \\ -\frac{1}{m_u} \end{bmatrix}, \quad B_f=\begin{bmatrix} 0 \\ -1 \\ 0 \\ \frac{c_t}{m_u} \end{bmatrix} \\ C=\begin{bmatrix} -\frac{k_s}{m_s} & 0 & -\frac{c_s}{m_s} & \frac{c_s}{m_s} \end{bmatrix}, \quad D=\frac{1}{m_s} \\ N_A=\begin{bmatrix} 0 & 0 & 0 & 0 \\ 0 & 0 & 0 & 0 \\ -\frac{k_s}{100m_s} & 0 & 0 & 0 \\ \frac{k_s}{100m_u} & 0 & 0 & 0 \end{bmatrix}, N_C=\begin{bmatrix} -\frac{k_s}{100m_s} & 0 & 0 & 0 \end{bmatrix}, M=I_4 \end{array}\right. \tag{52}$$

where $x = \begin{bmatrix} x_1 & x_2 & x_3 & x_4 \end{bmatrix}^T$, x_1 denotes the suspension deflection, x_2 is the tire deflection, x_3 is the speed of the car chassis, x_4 denotes the speed of the wheel assembly, y is the body vertical acceleration, and u is the active control input. The uncertainties are from a 1% time-varying perturbation in the stiffness of the suspension system. The parameter values of the suspension system are shown in Table 1.

Table 1. Values of quarter-car model parameters.

m_s	m_u	k_s	k_t	c_s	c_t
320 kg	40 kg	18 kN/m	200 kNs/m	1 kNs/m	10 Ns/m

Consider there is an isolated bump on an originally smooth road surface and the bump disturbance is given by

$$f(t) = \begin{cases} A_m \sin\left(\omega_f t\right), & \text{if } 0 \le t \le T_f, \\ 0, & \text{if } t \ge T_f, \end{cases} \tag{53}$$

where A_m, ω_f, and T_f represent the amplitude, angular frequency, and period of the vibration, respectively. Assume $A_m = 0.5$ m, $\omega_f = 12\pi$ rad/s (i.e., 6 Hz), which belongs to the frequency range $[4\text{ Hz},\ 8\text{ Hz}]$.

To mitigate the vibrations within $[4\text{ Hz},\ 8\text{ Hz}]$, a Butterworth band-pass filter with this band-pass frequency range is chosen. The corresponding parameters are

$$\begin{cases} A_F = \begin{bmatrix} -2.51327 & -3.55431 \\ 3.55431 & 0 \end{bmatrix} \times 10^1, \quad B_F = \begin{bmatrix} 1 \\ 0 \end{bmatrix} \\ C_F = \begin{bmatrix} 2.51327 & 0 \end{bmatrix} \times 10^1 \end{cases} \tag{54}$$

According to (9), we have

$$A_e = \begin{bmatrix} 0 & -3.55431 \\ 3.55431 & 0 \end{bmatrix} \times 10^1, \quad C_e = \begin{bmatrix} 2.51327 & 0 \end{bmatrix} \times 10^1, \tag{55}$$

Set the initial value γ_0 of the performance index γ as

$$\gamma_0 = 30. \tag{56}$$

Use the LQR method to determine an initial value for the control gains (L, K_e) of the observer and GEID estimator. The weighting matrices are selected as

$$Q = I_6, \quad R = 1. \tag{57}$$

which give

$$\begin{cases} L^{(1)} = \begin{bmatrix} -0.06202 & -0.0775 & -0.04142 & 3.57513 \end{bmatrix}^{\mathrm{T}} \times 10^1, \\ K_e^{(1)} = 7.69632 \times 10^1. \end{cases} \tag{58}$$

For the performance index (56) and the above control gains (58), an application of Theorem 2 gives

$$K_p^{(1)} = \begin{bmatrix} 1.3865 & -0.3866 & -0.2172 & -0.1001 \end{bmatrix} \times 10^4. \tag{59}$$

Further, set the decrease step γ_δ as

$$\gamma_\delta = 1. \tag{60}$$

For $K_p^{(1)}$ in (59), by trail and error, we find there are no feasible solutions of ($L^{(2)}$, $K_e^{(2)}$) to LMIs (33), and (34) of Theorem 1 due to the uncertainty blocks. Hence, the initial value ($L^{(1)}$, $K_e^{(1)}$) is still used to optimize the control gain K_p.

Thirteen iterations of Theorem 2 give

$$\gamma = 16 \tag{61}$$

and

$$K_p^{(14)} = \begin{bmatrix} 1.4003 & -0.3741 & -0.1962 & -0.1 \end{bmatrix} \times 10^4. \tag{62}$$

Then, we use the obtained gain $K_p^{(14)}$ in (62) to further optimize (L, K_e) by Theorem 1. For $\gamma = 15$ and $K_p = K_p^{(14)}$, an application of Theorem 1 gives

$$\begin{cases} L^{(15)} = [-0.29047 \; -0.41595 \; -2.38696 \; 0.46333]^{\mathrm{T}} \times 10^1, \\ K_e^{(15)} = 7.902321 \times 10^2. \end{cases} \tag{63}$$

Since there are no feasible solutions no matter for Theorem 1 or Theorem 2, we complete this design and use the following gains as the final control gains.

$$K_p = K_p^{(14)}, \quad L = L^{(15)}, \quad K_e = K_e^{(15)}. \tag{64}$$

The robust disturbance–rejection performance of the closed-loop uncertain control system satisfies

$$\|G\|_\infty < 15. \tag{65}$$

The response of the GEID-based suspension control system is shown in Figure 3. As we can see, the closed-loop system is robust stabilized in the presence of the time-varying parameter perturbation and disturbance. The influences of parameter perturbation and disturbance on the system output, i.e., the body acceleration, have been well suppressed by the EID estimate $\tilde{f}_e$ of the GEID estimator.

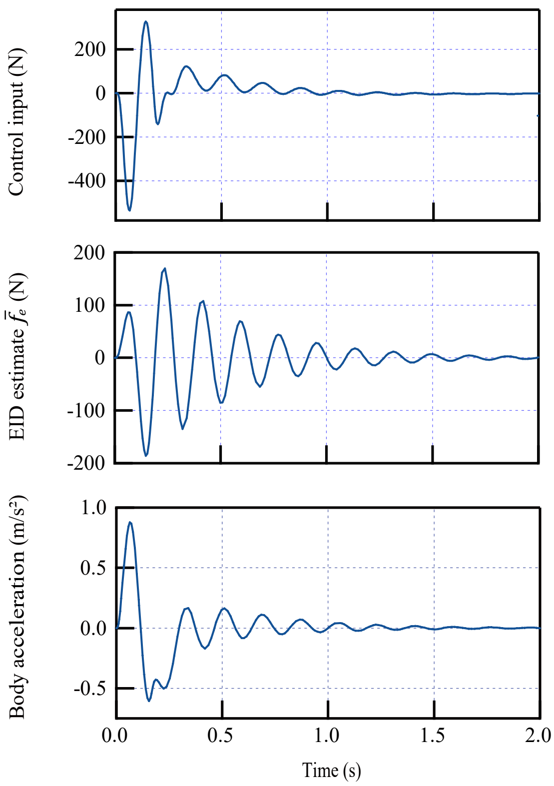

Figure 3. System response of the developed GEID-based control method.

6.2. Comparisons with Other Methods

In this section, the developed method is compared with the passive control and the state-feedback control [31] for the nominal plant of the suspension system with $\Delta A = 0$ and $\Delta C = 0$. The road disturbance is the same as (53).

First, the developed iterative design algorithm is applied. The band-pass filter is selected as the same as (54), which gives A_e and C_e in (55). Set the initial value γ_0 of the performance index γ as

$$\gamma_0 = 20. \tag{66}$$

The initial control gains are chosen as the same as (58). Set the decrease step γ_δ as

$$\gamma_\delta = 0.1. \tag{67}$$

For the initial performance index (66), the control gains (58) and the decrease step γ_δ (67) follow the developed iterative design algorithm by an alternate application of Theorems 1 and 2 until one of the two theorems has no feasible solutions. Finally, the H_∞ performance index is decreased to

$$\gamma = 4.6 \tag{68}$$

and the corresponding control gains K_p and (L, K_e) are given as follows.

$$\begin{cases} L = [-0.456379 \quad -0.42917 \quad -1.045224 \quad -7.954294]^{\mathrm{T}} \times 10^2, \\ K_e = 1.986 \times 10^3, \end{cases} \tag{69}$$

$$K_p = \begin{bmatrix} 1.7998 & -0.0003 & 0.0801 & -0.1 \end{bmatrix} \times 10^4. \tag{70}$$

For the comparison with the full-state feedback control [31], the optimal H_∞ performance index is 8.8, which is much greater than 4.6 of the developed method. Further, the corresponding gain of the state feedback control is

$$K_f = \begin{bmatrix} 0.0311 & 1.1096 & -0.0219 & 0.0214 \end{bmatrix} \times 10^5. \tag{71}$$

The passive control method is also compared with the developed method. A passive suspension system is actually an open-loop control system without any controller.

The magnitude-frequency characteristics of the transfer matrices from the disturbance $f(t)$ to the output $y(t)$ of the GEID-based, full-state feedback, and passive control are illustrated in Figure 4. The developed GEID-based control system includes an observer, a state-feedback controller, and a GEID estimator. In the sate-feedback control system, a full-state feedback controller is devised by minimizing the H_∞ disturbance–rejection performance index. However, it requires that all the states are available.

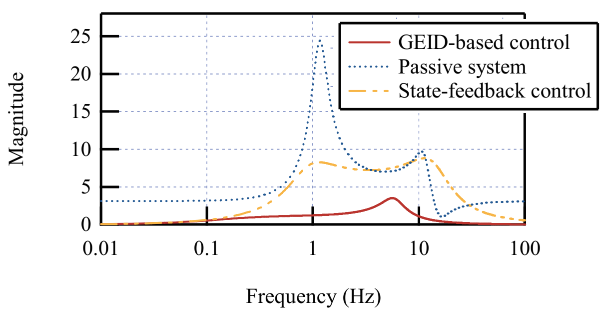

Figure 4. Magnitude-frequency characteristics of disturbance–rejection transfer function.

The output responses of the proceeding three methods are shown in Figure 5. The corresponding optimal H_∞ norm and the peak value of three control methods are given by Table 2.

As we can see, although the full-state feedback control is much better than the passive control, the developed GEID-based disturbance–rejection method has much better disturbance–rejection performance than the full-state feedback control. Moreover, the maximum vertical acceleration of the body is only about 0.018 m/s^2.

All in all, the developed iterative design method provides the best disturbance–rejection performance over the frequency band [4 Hz, 8 Hz].

On the other hand, the full-state feedback control requires all states of the active suspension system, which may be costly and even difficult to achieve. All in all, the developed GEID-based control method has significant advantages over the state-feedback control method.

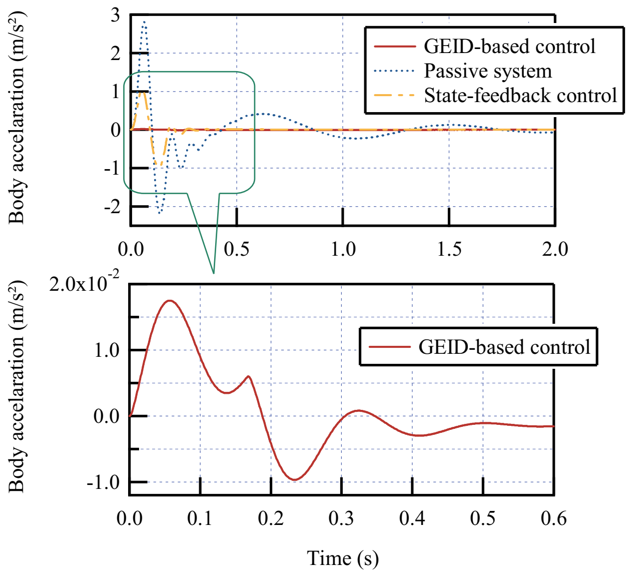

Figure 5. Output response of body acceleration.

Table 2. The optimal H_∞ norm and the peak value of three control methods.

Index\Methods	GEID-Based Control	Passive System	State-Feedback Control
Optimal $\boldsymbol{H_\infty}$ norm	4.6	15	8.8
Peak value	0.017	2.808	1.044

7. Conclusions

This paper presented an iterative design algorithm for the robust disturbance–rejection control of uncertain systems, which removed the constraints due to the widely used commutative condition. First, two state-space models were built for the closed-loop uncertain control system. By the bounded real lemma, the robust H_∞ disturbance–rejection performance index was derived for performance optimization. Further, a robust stability condition was obtained. An iterative design algorithm was given, which guaranteed both robust stability and disturbance-rejection performance, Moreover, the gains of the state-feedback controller, the state observer, and the GEID estimator can be easily obtained by using the LMI-based technique. Finally, by a case study of a suspension control system of modern vehicles and comparisons with other methods, the effectiveness and advantages of the developed GEID-based iterative design method were clarified.

Author Contributions: Conceptualization, P.Y.; methodology, P.Y. and J.L.; software, J.L. and N.L.; validation, J.L., N.L. and H.Z.; formal analysis, J.L. and C.L.; investigation, N.L., H.Z. and C.L.; resources, J.L., N.L. and H.Z.; data curation, J.L.; writing—original draft preparation, P.Y. and J.L.; writing—review and editing, J.L. and N.L.; visualization, J.L. and N.L.; supervision, P.Y.; project administration, P.Y.; funding acquisition, P.Y. and C.L. All authors have read and agreed to the published version of the manuscript.

Funding: This work was supported by the National Natural Science Foundation of China under Grants 62003010 and 62273012, the Beijing Natural Science Foundation under Grant 4212933, and the Scientific Research Project of Beijing Educational Committee under Grant KM202110005023.

Data Availability Statement: The data are contained within the article.

Conflicts of Interest: The authors declare no conflict of interest.

Appendix A

This appendix contains a table of variable and acronym definitions used in the paper.

Table A1. Acronyms.

Acronyms	Definition
EID	Equivalent-input-disturbance
GEID	Generalized equivalent-input-disturbance
LMIs	Linear matrix inequalities
LQR	Linear quadratic regulator

Table A2. Known parameters or variables.

Known Parameters or Variables	Definition
A	System matrix
B	Input matrix
C	Output matrix
D	Direct transmission matrix
N_A,N_C and M	known real constant matrices of parameter uncertainties
B_f	Disturbance input channel
$F(s)$	General filter
K_p	Feedback control gain
L	Observer gain
K_e	GEID control gain

References

1. Liu, K.Z.; Yao, Y. *Robust Control: Theory and Applications*; Wiley: Hoboken, NJ, USA, 2016.
2. Yang, J.; Cui, H.; Li, S.; Zolotas, A. Optimized active disturbance rejection control for DC-DC buck converters with uncertainties using a reduced-order GPI observer. *IEEE Trans. Circuits Syst. Regul. Pap.* **2018**, *65*, 832–841. [CrossRef]
3. Xu, B.; Zhang, L.; Ji, W. Improved non-singular fast terminal sliding mode control with disturbance observer for PMSM drives. *IEEE Trans. Transp. Electrif.* **2021**, *7*, 2753–2762. [CrossRef]
4. Chen, W.; Yang, J.; Guo, L.; Li, S. Disturbance observer-based control and related methods-an overview. *IEEE Trans. Ind. Electron.* **2016**, *63*, 1083–1095. [CrossRef]
5. Miyamoto, K.; She, J.H.; Nakano, S.; Sato, D.; Chen, Y.L. Active structural control of base-Isolated building using equivalent-input-disturbance approach with reduced-order state observer. *J. Dyn. Syst. Meas. Control.* **2022**, *144*, 1081–1095. [CrossRef]
6. Zhou, Y.; She, J.H.; Wang, F.; Iwasaki, M. Disturbance rejection for stewart platform based on integration of equivalent-input-disturbance and sliding-mode control methods. *IEEE/ASME Trans. Mechatron.* **2023**, 1–11. [CrossRef]
7. Stobart, R.K.; Kuperman, A.; Zhong, Q.C. Uncertainty and disturbance estimator-based control for uncertain LTI-SISO systems with state delays. *J. Dyn. Syst. Meas. Control.* **2011**, *133*, 024502. [CrossRef]
8. Wu, Y.; Mahmud, M.H.; Zhao, Y.; Mantooth, H.A. Uncertainty and disturbance estimator-based robust tracking control for dual-active-bridge converters. *IEEE Trans. Transp. Electrif.* **2020**, *6*, 1791–1800. [CrossRef]
9. Choi, Y.; Yang, K.; Chung, W.K.; Kim, H.R.; Suh, I.H. On the robustness and performance of disturbance observers for second-order systems. *IEEE Trans. Autom. Control.* **2003**, *48*, 315–320. [CrossRef]
10. Li, M.; Yan, T.; Mao, C.; Wen, L.; Zhang, X.; Huang, T. Performance-enhanced iterative learning control using a model-free disturbance observer. *IET Control. Theory Appl.* **2021**, *15*, 978–988. [CrossRef]
11. Xie, Y.; Qiao, J.; Yu, X.; Guo, L. Dual-disturbance observers-based control for a class of singularly perturbed systems. *IEEE Trans. Syst. Man Cybern. Syst.* **2022**, *52*, 2423–2434. [CrossRef]
12. Cui, Y.; Qiao, J.; Zhu, Y.; Yu, X.; Guo, L. Velocity-tracking control based on refined disturbance observer for gimbal servo system with multiple disturbances. *IEEE Trans. Ind. Electron.* **2022**, *69*, 10311–10321. [CrossRef]

13. Wang, L.X.; Zhao, D.X.; Zhang, Z.X.; Liu, Q.; Liu, F.C.; Jia, T. Model-free linear active disturbance rejection output feedback control for electro-hydraulic proportional system with unknown dead-zone. *IET Control. Theory Appl.* **2021**, *15*, 2081–2094. [CrossRef]
14. Li, S.; Yang, J.; Chen, W.; Chen, X. Generalized extended state observer based control for systems with mismatched uncertainties. *IEEE Trans. Ind. Electron.* **2012**, *59*, 4792–4802. [CrossRef]
15. Castillo, A.; Garcia, P.; Sanz, R.; Albertos, P. Enhanced extended state observer-based control for systems with mismatched uncertainties and disturbances. *ISA Trans.* **2018**, *73*, 1–10. [CrossRef]
16. She, J.H.; Fang, M.; Ohyama, Q.; Hashimoto, H.; Wu, M. Improving disturbance-rejection performance based on an equivalent-input-disturbance approach. *IEEE Trans. Ind. Electron.* **2008**, *55*, 380–389. [CrossRef]
17. Du, Y.; Cao, W.; She, J.H.; Wu, M.; Fang, M.; Kawata, S. Disturbance rejection and predictive control for systems with input and output delays. *IEEE Trans. Syst. Man Cybern. Syst.* **2022**, *52*, 4589–4599. [CrossRef]
18. Huang, G.; She, J.H.; Fukushima, E.F.; Zhang, C.; He, J. Robust reconstruction of current sensor faults for PMSM drives in the presence of disturbances. *IEEE/ASME Trans. Mechatronics* **2019**, *24*, 919–2930. [CrossRef]
19. Yu, P.; Liu, K.Z.; Wu, M.; She, J.H. Analysis of equivalent-input-disturbance-based control systems and a coordinated design algorithm for uncertain systems. *Int. J. Robust Nonlinear Control.* **2021**, *31*, 1755–1773. [CrossRef]
20. Liu, R.J.; Liu, G.; Wu, M.; Xiao, F.; She, J.H. Robust disturbance rejection based on equivalent-input-disturbance approach. *IET Control. Theory Appl.* **2013**, *7*, 1261–1268. [CrossRef]
21. Du, Y.W.; Cao, W.H.; She, J.H.; Wu, M.; Fang, M.X.; Seiichi, K. Disturbance rejection and robustness of improved equivalent-input-disturbance-based system. *IEEE Trans. Cybern.* **2022**, *52*, 8537–8546. [CrossRef]
22. Yu, P.; Liu, K.Z.; Wu, M.; She, J.H. Improved equivalent-input-disturbance approach based on H_∞ control. *IEEE Trans. Ind. Electron.* **2020**, *67*, 8670–8679. [CrossRef]
23. Yu, P.; Liu, K.Z.; Li, X.L.; Yokoyama, M. Robust control of pantograph-catenary system: Comparison of 1-DOF-based and 2-DOF-based control systems. *IET Control. Theory Appl.* **2021**, *15*, 2258–2270. [CrossRef]
24. Levine, W.S. *The Control Handbook*; CRC Press: Boca Raton, FL, USA, 1996.
25. Sands, T.; Bollino, K.; Kaminer, I.; Healey, A. Autonomous minimum safe distance maintenance from submersed obstacles in ocean currents. *J. Mar. Sci. Eng.* **2018**, *6*, 98. [CrossRef]
26. Sands, T. Virtual sensoring of motion using pontryagin's treatment of hamiltonian systems. *Sensors* **2021**, *21*, 4603. [CrossRef]
27. Yu, P.; Liu, K.Z.; She, J.H.; Wu, M.; Nakanishi, Y. Robust disturbance rejection for repetitive control systems with time-varying nonlinearities. *Int. J. Robust Nonlinear Control* **2019**, *29*, 1597–1612. [CrossRef]
28. Rantzer, A. On the Kalman-Yakubovich-Popov Lemma for Positive Systems. *IEEE Trans. Autom. Control.* **2016**, *61*, 1346–1349. [CrossRef]
29. Petersen, I.R.; Hollot, C.V. A riccati equation approach to the stabilization of uncertain linear systems. *Automatica* **1986**, *22*, 397–411. [CrossRef]
30. Yu, L. *Robust Control-Linear Matrix Inequality Method*; Tsinghua University Press: Beijing, China, 2002.
31. Sun, W.C.; Gao, H.; Kaynak, O. Finite frequency H_∞ control for vehicle active suspension systems. *IEEE Trans. Control. Syst. Technol.* **2011**, *19*, 416–422. [CrossRef]